Original Article



MicroRNA-1912 regulates cholesterol homeostasis by targeting PCSK9

Chan Joo Lee,^{1,6} Myeongjune Go,^{2,6} Sae-Bom Jeon,² Sun-Ho Lee,² Dongkook Min,³ So Hee Park,² Seunghyun Lee,^{2,4,7} and Sahng Wook Park^{2,5,7}

¹Division of Cardiology, Severance Cardiovascular Hospital, Yonsei University College of Medicine, 50-1 Yonsei-ro, Seodaemun-gu, Seoul 03722, South Korea; ²Department of Biochemistry and Molecular Biology, Yonsei University College of Medicine, 50-1 Yonsei-ro, Seodaemun-gu, Seoul 03722, South Korea; ³Krantz Family Center for Cancer Research, Massachusetts General Hospital Cancer Center, Charlestown, MA 02129, USA; ⁴Division of Cardiology, Department of Medicine, Johns Hopkins University School of Medicine, Baltimore, MD 21205, USA; ⁵Department of Biochemistry and Molecular Biology, Institute of Genetic Science, Yonsei University College of Medicine, Seoul 03722, South Korea

Proprotein convertase subtilisin/kexin type 9 (PCSK9) binds to low-density lipoprotein (LDL) receptor (LDLR) and promotes degradation of LDLR, regulating cholesterol homeostasis. Previous studies have reported several microRNAs (miR-NAs) that regulate PCSK9 expression; however, evidence for these effects in animal models remains controversial. This study aimed to explore miRNA candidates for PCSK9 regulation and to validate the most potent miRNA for this regulation in vivo. Bioinformatic algorithms identified miRNAs regulating PCSK9, with miR-224 and miR-1912 showing a high probability of targeting PCSK9. Treatment with miR-224 and miR-1912 significantly reduced PCSK9 mRNA and protein levels and led to an increase in LDLR protein expression, resulting in increased uptake of LDL particles in HepG2 cells, with miR-1912 showing a greater effect than miR-224. Specific interactions of miR-1912 and miR-224 with the 3' untranslated region (UTR) of PCSK9 mRNA were confirmed by a luciferase reporter assay and site-directed mutagenesis analysis of the predicted seed region. In transgenic mice expressing liver-specific human PCSK9 with its 3' UTR, administration of miR-1912 mimics resulted in a reduction of plasma total cholesterol levels as determined by fast protein liquid chromatography following hepatic delivery. These findings highlight miR-1912 as a promising therapeutic candidate for hypercholesterolemia via targeted, post-transcriptional regulation of PCSK9.

INTRODUCTION

Proprotein convertase subtilisin/kexin type 9 (PCSK9), a member of protein convertases, promotes the breakdown of the low-density lip-oprotein (LDL) receptor (LDLR). LDLR is endocytosed into cells when it binds to lipoproteins on the surface of a cell and is recycled to a cell membrane after dissociation from bound lipoproteins in the low-pH environment in endosomes. ^{1,2} PCSK9 binds to the first epidermal growth factor-like repeat A domain of LDLR, and the PCSK9-LDLR complex is endocytosed into cells, even without binding lipoproteins to LDLR. PCSK9-LDLR complex is directed to the lysosome and degraded instead of being recycled. ³ The gain-of-function mutation of *PCSK9* reduces the expression of LDLR, resulting in

an elevation of blood LDL cholesterol concentration. ⁴ Conversely, the loss of function of *PCSK9* reduces LDLR destruction, resulting in increased absorption of LDL cholesterol into the cell and ultimately lowering the incidence of coronary artery disease. ⁵ By altering the expression level of LDLR, the qualitative and quantitative change in PCSK9 affects cholesterol-related diseases.

Cellular cholesterol homeostasis is regulated by SREBP-2.⁶ Statins inhibit cholesterol synthesis via 3-hydroxy-3-methylglutaryl-CoA (HMG-CoA) reductase inhibition, leading to SREBP-2 activation and subsequent LDLR upregulation, increasing LDL reuptake. Paradoxically, the expression of PCSK9, which reduces LDLR levels, is also upregulated by activated SREBP-2, and this parallel induction of LDLR and PCSK9 hinders the blood cholesterol-lowering effect of statins.⁷⁻⁹ Statins increase LDLR expression and lower blood cholesterol levels more effectively in *PCSK9* knockout mice than wild-type (WT) mice.¹⁰ Based on this experimental background, monoclonal antibodies that inhibit PCSK9 were developed, and these drugs have proven to be effective in lowering blood cholesterol and reducing clinical events in patients with acute coronary syndrome or familial hypercholesterolemia.¹¹⁻¹³ Recently, small interfering RNA (siRNA) targeting *PCSK9* was also developed as a drug.¹⁴

MicroRNAs (miRNAs) are small non-coding RNAs that consist of ~22 nucleotides, bind to the 3' untranslated region (UTR) of target mRNAs, and regulate the post-transcriptional expression of target genes. Emerging evidence suggests that the altered expression of miRNAs may be involved in the pathogenesis of several human

Received 17 December 2024; accepted 5 June 2025; https://doi.org/10.1016/j.omtn.2025.102589.

⁶These authors contributed equally

⁷These authors contributed equally

Correspondence: Seunghyun Lee, Johns Hopkins University, Baltimore, MD 21205, USA.

E-mail: slee600@jhmi.edu

Correspondence: Sahng Wook Park, Yonsei University College of Medicine, Seoul 03722, South Korea.

E-mail: SWPARK64@yuhs.ac



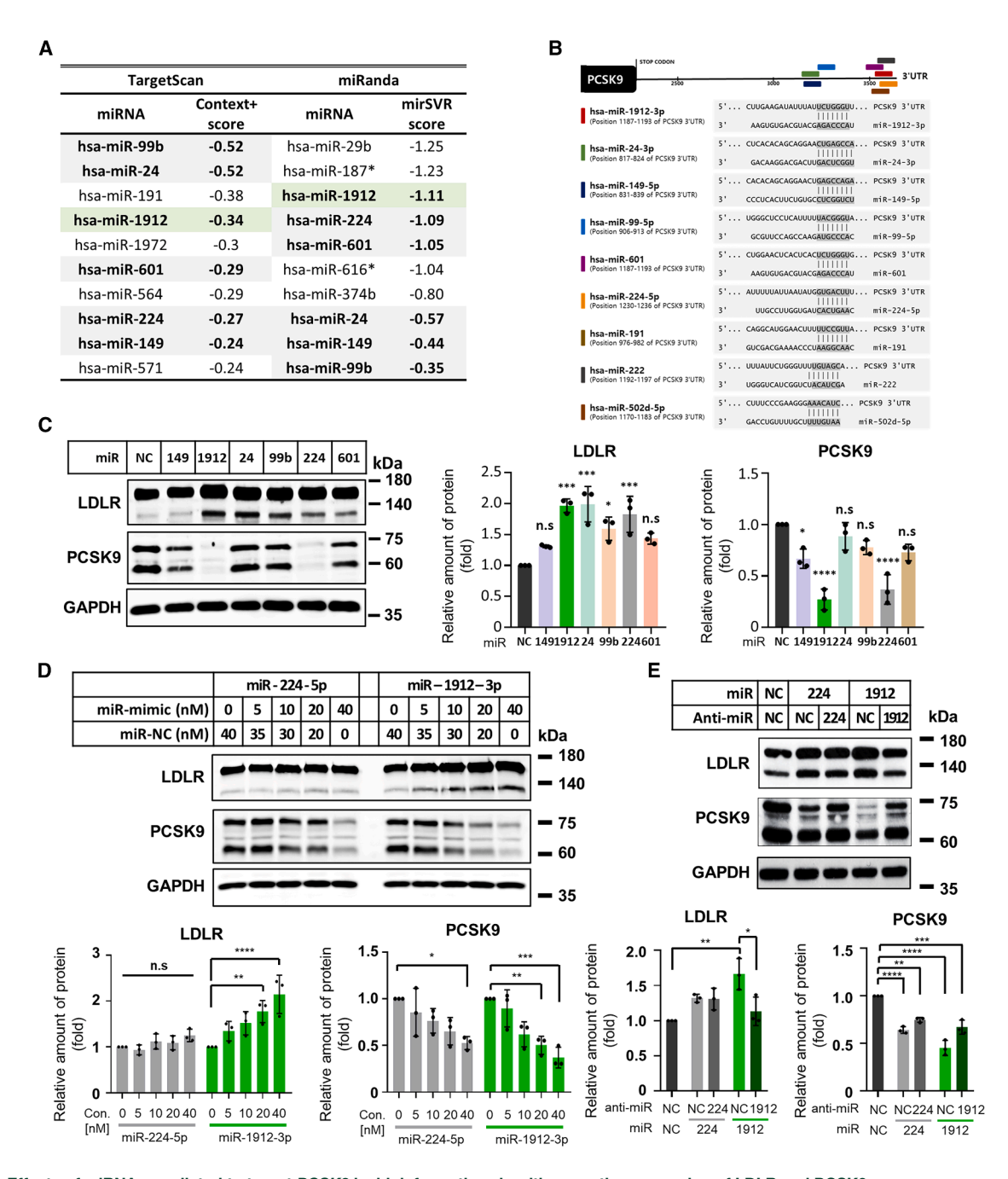


Figure 1. Effects of miRNAs predicted to target *PCSK9* by bioinformatics algorithms on the expression of LDLR and PCSK9
(A) TargetScan and miRanda algorithms predicted several miRNAs as candidates for targeting PCSK9. Overlapping miRNAs are indicated in bold font. (B) Schematic

The candidates were selected with online computational algorithms TargetScan, miRs that bind to the PCSK9-3'-UTR and each of binding sites and sequence are shown. The candidates were selected with online computational algorithms TargetScan, miRDB, and miRTarBase database. (C) On day 0, HepG2 cells were transfected with each miRNA mimic at a final concentration of 40 nM, as described in materials and methods. On day 1, the cells were switched to fresh medium A, supplemented with 10% delipidated serum (DLPS). On day 2, cells were switched to fresh medium A supplemented with 10% DLPS, 0.1 µM of rosuvastatin, and 0.05 mM of sodium mevalonate. On day 3, cells were harvested, and immunoblot analysis was carried out with polyclonal antibodies against PCSK9 and low-density lipoprotein receptor (LDLR). GAPDH was used as a loading control. Statistical analysis of protein expression was performed using one-way ANOVA, with the results of miR-NC as the reference. (D) On day 0, HepG2 cells were transfected with the indicated concentrations of miR-224-3p or miR-1912-3p in 12-well plates as described previously. The total amount of transfected miRNA (legend continued on next page)

diseases, such as Alzheimer's disease, type 1 diabetes, cancer, cardiovascular, inflammatory, and genetic diseases. 16-18 With the recent development of various in vivo miRNA delivery modalities, including nanomaterials and exosomes, the practical application of exogenous miRNAs for therapeutic purposes has become feasible. 19,20 In the research era of cholesterol metabolism, Rayner et al. have discovered that miR-33 represses the expression of the adenosine triphosphate-binding cassette transporter, which has the role of secreting cellular cholesterol out of the cell in the form of apolipoprotein A1.²¹ It has been proven that miR-122 is involved in the metabolism of fatty acids and cholesterol.²² miRNA-370 is also known to be involved in the oxidation process of fatty acids by regulating miR-122 expression.²² However, research on miRNAs, particularly targeting the PCSK9 gene, has not produced any apparent results. Naeli et al. and Salerno et al. reported several candidate miRNAs targeting PCSK9; however, the effect of these miRNAs in animal experiments is controversial. 23,24 The aim of this study is to identify the efficacy of the most effective miRNA among those predicted to reduce PCSK9 expression in vitro and in vivo.

RESULTS

Effects of miR-224 and miR-1912 on the expression of LDLR and PCSK9 in HepG2 cells

In the present study, miRNAs targeting PCSK9 were screened using an online miRNA database. miRNAs with lower Context+ scores in TargetScan or lower mirSVR scores in miRanda were more favorable candidates as regulators of PCSK9 and are listed in the order of score (Figure 1A). Six miRNAs, hsa-miR-149-5p, hsa-miR-1912-3p, hsamiR-24-3p, hsa-miR-99b, hsa-miR-224-5p, and hsa-miR-601, were selected for further analysis. hsa-miR-224-5p has been commonly mentioned as one of the most effective miRNAs targeting PCSK9 in previous research, 23,24 thus hsa-miR-224-5p was used as a reference in this experiment. We represented the schematic diagram of the PCSK9-3'-UTR part targeted by predicted miRNAs (Figure 1B). To determine whether the selected miRNAs affected PCSK9 expression in vitro, the levels of PCSK9 and LDLR were evaluated after the transient transfection of each miRNA in HepG2 cells. Among the predicted miRNAs, hsa-miR-1912-3p most effectively reduced the expression of pro-PCSK9 (73 kDa) and active PCSK9 (58 kDa), with a marked increase in LDLR expression (Figure 1C). hsa-miR-149-5p reduced the amount of PCSK9; however, it did not affect the LDLR. The effects of hsa-miR-24-3p, hsa-miR-99b, and hsa-miR-601 on PCSK9 and LDLR levels were relatively small compared with those of hsa-miR-224-5p and hsa-miR-1912-3p. Accordingly, hsa-miR-224-5p and hsa-miR-1912-3p were selected for further evaluation of their potential to regulate PCSK9 and cellular cholesterol metabolism via LDLR. The effects of hsa-miR-1912-3p on PCSK9 reduction and LDLR protein increase were dose-dependent, showing significant impact up to a final concentration of 40 nM (Figure 1D), while hsa-miR-224-5p exhibited a weaker dose-dependent reduction in PCSK9 protein levels and minimal increase in LDLR protein levels. When cells were co-transfected with miRNAs and antisense oligonucleotides (anti-miR miRNA inhibitors) that silenced the action of miRNAs, the effects of hsa-miR-1912-3p on PCSK9 and LDLR proteins were more significantly attenuated than hsa-miR-224-5p (Figure 1E). Collectively, these findings demonstrate that hsa-miR-1912-3p has a greater potential to control cholesterol metabolism by directly inhibiting PCSK9 expression compared to hsa-miR-224-5p.

miR-1912 targets the 3' UTR of PCSK9 mRNA

The genomic locus of hsa-miR-1912-3p is located in intron 2 of serotonin receptor 2C (5-hydroxytryptamine receptor 2C; HTR2C) on the X chromosome (Figure 2A). The hsa-miR-1912-3p binding sites of PCSK9-3'-UTR were conserved only across primates (Figure 2B). Those in rodents differ by two nucleotides. The sequences, which are responsive to the seed region of mature human miR-1912, are conserved across primates. However, the mature forms of hsa-miR-1912-3p differed in length among species (Figure 2C). The expressions of hsa-miR-1912-3p and its host gene, HTR2C, were examined using a TaqMan miRNA assay and quantitative real-time PCR (qRT-PCR). Ct values were greater than 35, suggesting that hsa-miR-1912-3p and HTR2C were not expressed in HepG2 cells (data not shown). Therefore, we focused on the possibility of using this miRNA as an exogenous therapeutic agent rather than for endogenous regulation. To verify whether miRNAs affect PCSK9 expression via the 3' UTR of PCSK9 mRNA, a luciferase reporter assay was carried out using pLightSwitch_PCSK9_3UTR, which contains the entire 3' UTR of PCSK9 mRNA flanked downstream of the Renilla luciferase reporter gene (Figure 2D). The sequences of the putative binding sites for hsamiR-1912-3p or hsa-miR-224-5p and unrelated sites are shown in Figures 2E and S1A, respectively, and the locations of the introduced mutations are indicated. Co-transfection of HEK293 cells with the WT construct and hsa-miR-1912-3p or hsa-miR-224-5p resulted in decreased luciferase activity compared to cells co-transfected with the control miRNA mimic in Figures 2F and S1B. When mutations were introduced to putative binding regions for miRNAs in the 3' UTR by site-directed mutagenesis (Mut-1912-A, -1912-B, and -1912-C in Figure 2F and Mut-224-A, -224-B, and -224-C in Figure S1B), luciferase activity was unchanged or slightly decreased by miRNAs. However, introducing the mutation in the region unrelated to the predicted binding region in the 3' UTR showed no effect on reducing the WT reporter activity by miRNAs (Mut-1912-D in Figure 2F and Mut-224-D in Figure S1B). To further investigate the intracellular interaction of hsa-miR-1912-3p and its target mRNA, an AGO2 pull-down assay was conducted in HepG2 cells. Consistent with the luciferase assay, a distinct interaction with PCSK9 mRNA was detected following treatment with high levels

mimic was adjusted to 40 nM per well with miR-NC. Cells were incubated and harvested, and immunoblot analysis was performed. (E) On day 0, HepG2 cells were transfected with the indicated miRNA mimics at a final concentration of 40 nM and the indicated antisense oligonucleotides against miRNAs (anti-miR) at a final concentration of 100 nM, as described previously. Statistics were performed using one-way ANOVA with Tukey's post hoc test. Each value represents the mean \pm SD (*p < 0.05, **p < 0.01, ***p < 0.001, and ****p < 0.0001; n.s, not significant).

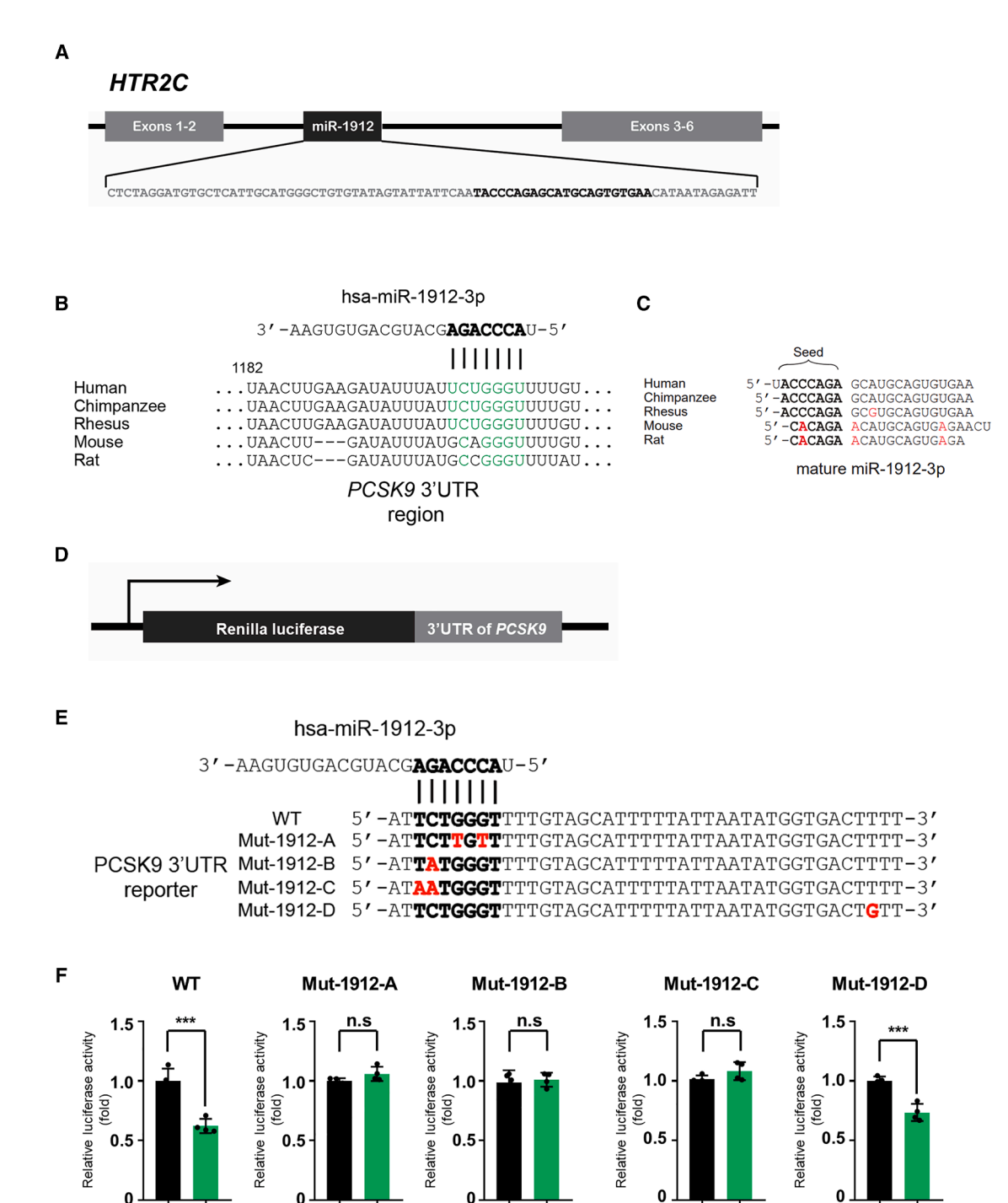


Figure 2. miR-1912 targets PCSK9 directly

miR

NC 1912

(A) Schematic representation of the miR-1912 coding sequence in the HTR2C (5-hydroxytryptamine receptor 2C) gene. Sequences encoding the pre-miRNA are shown, with mature miR-1912 sequences highlighted in bold. (B) 3' UTR sequences of PCSK9 flanking miR-1912 target sites are aligned among humans, chimpanzees, rhesus monkeys, mice, and rats. The conserved sequences are shown in bold. (C) Sequences of mature miR-1912 are aligned across species. Conserved sequences in the seed regions are shown in bold. HTR2C. (D) Schematic representation of the luciferase reporter vector harboring the PCSK9 -3'-UTR fragment (gray box). (E) Interaction between miR-1912

NC 1912

miR

NC 1912

miR

NC 1912

miR

(legend continued on next page)

miR

NC 1912

of hsa-miR-1912-3p, supporting the conclusion that *PCSK9* mRNA is direct target of hsa-miR-1912-3p in a cells (Figure S2). Together, these results suggest that miR-1912 reduces the expression of PCSK9 by specifically targeting the corresponding regions of *PCSK9* mRNA as well as hsa-miR-224-5p.

miR-1912 targets *PCSK9* more effectively in the HepG2 cell line than miR-224

Changes in PCSK9 and LDLR expression were validated by RTqPCR (Figures 3A and 3B). The amount of PCSK9 mRNA was significantly decreased by hsa-miR-1912-3p compared to hsa-miR-224-5p. Interestingly, while hsa-miR-224 did not alter LDLR mRNA levels, hsa-miR-1912-3p increased LDLR mRNA levels. This change in LDLR mRNA levels could result from either the direct action of miRNAs or indirectly from miRNA-mediated alterations in cholesterol metabolism via changes in PCSK9 expression. These findings are also supported by microarray results. Microarray analysis of hsa-miRNA-1912-3p-transfected HepG2 cells revealed that the expression levels of 1,522 genes were significantly altered compared to the control, with 526 genes overlapping with gene changes caused by hsa-miR-224-5p (Figures S3A and S3B). Gene ontology analysis of these genes revealed enrichment in the cholesterol homeostasis pathway (Figure S3C). When genes were grouped according to their roles in cholesterol regulation, a more pronounced effect of hsa-miR-1912-3p on LDLR mRNA regulation was observed. Immunoblot analysis revealed that these miRNAs reduced PCSK9 protein levels regardless of cholesterol treatment and effectively blocked the rosuvastatin-induced upregulation of PCSK9 (Figures 3C-3E). Accordingly, LDLR increased. We confirmed that these changes were more apparent for hsa-miR-1912-3p than for hsa-miR-224-5p. To investigate whether changes in PCSK9 expression by miRNAs affected cholesterol metabolism via LDLR, the effect of miRNAs on LDL cholesterol uptake was evaluated. After miRNA transfection, the cells were incubated in a medium containing fluorescently tagged LDL (Dil-LDL). Fluorescence microscopy images were obtained, and the uptake of Dil-LDL was measured using fluorescence-activated cell sorting (FACS) analysis. Compared to miR-NC-transfected cells, both hsa-miR-224-5p- and hsa-miR-1912-3p-transfected cells contained more red Dil-LDL particles (Figure 3F). When a histogram of fluorescence intensity was constructed using FACS, the histogram of the selected miRNA-transfected cells (red line) shifted to the right, indicating a relative increase in cellular LDL cholesterol uptake (Figure 3G). hsa-miR-224-5p increased the fluorescence intensity by 20% but was not statistically significant. However, hsa-miR-1912-3p demonstrated a significant increase in Dil-LDL uptake by 70% or greater (Figure 3H). These data suggest that hsa-miR-1912-3p is a more effective PCSK9 inhibitor than hsa-miR-224-5p.

Characterization of liver-specific human PCSK9-3'-UTR overexpression mice

To verify the regulatory roles of hsa-miR-1912-3p in PCSK9 expression in vivo, we generated liver-specific human PCSK9-3'-UTR transgenic (TG) mice ($hPCSK9^{TG}$). First, we established $hPCSK9^{TG}$ mice in which human PCSK9, including the 3' UTR cloned plasmid, was microinjected into the mouse embryo. The PCR-based genotyping strategy is shown in Figure 4A. Alb-Cre lines expressed in hepatocytes have the albumin promoter, which directs transcription of Cre-recombinase, allowing expression of *PCSK9-3*'-UTR in the liver. Figure 4B illustrates that the $hPCSK9^{TG}$ mice were crossbred with Alb-Cre mice to generate Alb-Cre/hPCSK9-3'-UTR TG mice (hPCSK9^{TG(Alb-Cre)}). Proteins were extracted from the livers of mice of each genotype, and the expression of human PCSK9 and murine Ldlr was confirmed by immunoblotting (see Figure S4B). Subsequently, we examined the phenotype of the established $hPCSK9^{TG(Alb-Cre)}$ mice. There was no difference in body weight between Alb-Cre and hPCSK9^{TG(Alb-Cre)} mice fed a normal chow diet (Figure 4C). To determine the expression levels of PCSK9 and Ldlr, proteins and RNA were isolated from the livers of Alb-Cre and $\hat{hPCSK9^{TG(Alb-Cre)}}$ mice. Immunoblot analysis showed increased expression of human PCSK9 in the livers of hPCSK9^{TG(Alb-Cre)} mice compared to that in Alb-Cre mice, as expected. We also found that overexpression of human PCSK9 affected the expression of mouse Ldlr, as evidenced by a reduction in mouse Ldlr in $hPCSK9^{TG(Alb-Cre)}$ mice (Figure 4D). The mRNA expression levels of PCSK9 and Ldlr were determined by qRT-PCR. High levels of human PCSK9 were found in $hPCSK9^{T\dot{G}(A\dot{l}b-Cre)}$ mice but not in Alb-Cre mice. However, the difference in mRNA levels of Ldlr was not significant (Figure 4E), and plasma cholesterol concentration was higher in $hPCSK9^{\bar{T}G(Alb-Cre)}$ mice than in Alb-Cre mice (Figure 4F). These results show that human PCSK9 is overexpressed in the liver of hPCSK9^{TG(Alb-Cre)} mice and that human PCSK9 can influence cholesterol concentrations by regulating the amount of mouse Ldlr protein.

miR-1912 targets PCSK9-induced cholesterol dysregulation in vivo

To determine whether hsa-miR-1912-3p exerts its effects by directly targeting the human *PCSK9*-3'-UTR, we injected hsa-miR-1912-3p mimics into the tail veins of *hPCSK9*^{TG(Alb-Cre)} mice. *hPCSK9*^{TG(Alb-Cre)} mice were injected with 4 mg/kg miR-negative control (NC) or hsa-miR-1912-3p mimic, and the blood and liver were isolated 24 h later. No mice died after miR injection, and there was no difference in collagen area observed in Masson's trichrome staining and Sirius red staining of liver tissue from mice injected with either miR-NC or hsa-miR-1912-3p (Figure S5). There was no difference in the liver weight to body weight ratio (Lwt/Bwt) between mice injected with miR-NC and hsa-miR-1912-3p

and PCSK9-3'-UTR predicted by TargetScan. The interaction is highlighted in bold font, and mutant vectors with point mutations inside or outside the binding region are shown. The name of each construct is shown on the left side. (F) Relative luciferase activity after co-transfection of PCSK9-3'-UTR vectors with miR-1912 (n = 4/group). The luciferase activities of the indicated PCSK9-3'-UTR reporter constructs in cells co-transfected with miR-1912 were normalized to those in cells co-transfected with miR-NC. Statistics were performed using a two-tailed unpaired Student's t test with a Shapiro-Wilk test. Each value represents the mean \pm SD (***p < 0.001; n.s, not significant).

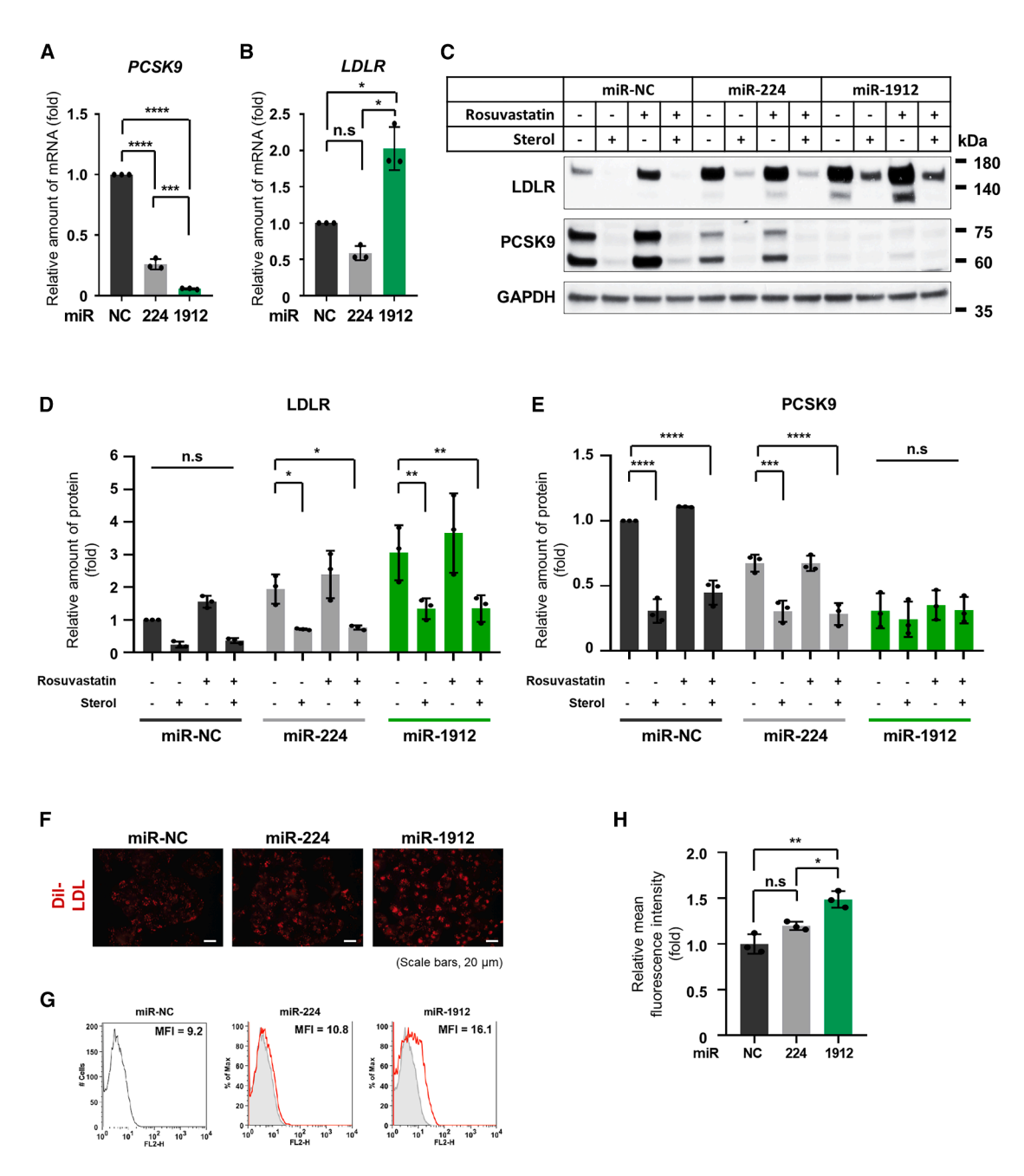


Figure 3. miR-1912 targets PCSK9 more effectively in the HepG2 cell line than miR-224

(A and B) HepG2 cells were transfected with miRNA at a final concentration of 40 nM. On day 1, the cells were switched to fresh medium A, supplemented with 10% DLPS. On day 2, cells were switched to fresh medium A supplemented with 10% DLPS, 0.1 μ M rosuvastatin, and 0.05 mM sodium mevalonate. On days 3 and 16 h after incubation, total RNAs from cells were prepared and subjected to reverse transcription and RT-qPCR. Each value represents the amount of mRNA relative to cells transfected with miRNC, which was arbitrarily defined as 1. miR-NC was used as a negative control miRNA mimic. Values represent the mean \pm SD (*p < 0.05). (C) After cells were transfected, the medium was replaced with fresh medium. On day 2, cells were switched with 10% DLPS, 0.1 mM rosuvastatin, and 0.05 mM sodium mevalonate, or 1 μ g/mL 25-hydroxycholesterol and 10 μ g/mL cholesterol, as indicated in the figure. After 16 h of incubation, on day 3, the cells were harvested, and immunoblot analysis was performed. (D and E) Quantitative graph of densitometry analysis for LDLR and PCSK9 images in Figure 3C. Data were normalized to GAPDH and statistically analyzed based on results from each miRNA treatment group without rosuvastatin and without sterol. (F) Fluorescence microscopy images of Dil-LDL uptake by HepG2 cells. HepG2 cells were transfected with miR-NC, miR-224, or miR-1912 mimics at a final concentration of 40 nM. After 16 h of incubation, on day 3, the cells were switched to fresh medium

(legend continued on next page)

(Figure 5A). Immunoblot analysis showed that human PCSK9 expression was significantly reduced in hsa-miR-1912-3pinjected hPCSK9^{TG(Alb-Are)} mice compared to miR-NC-injected hPCSK9^{TG(Alb-Cre)} mice (Figure 5B). Conversely, mouse Ldlr expression showed a significant increase. Lipoprotein fractions from the pooled plasma of Alb-Cre and hPCSK9^{TG(Alb-Cre)} male mice injected with miR-NC or hsa-miR-1912-3p were isolated by ultracentrifugation and separated by fast-performance liquid chromatography (FPLC). In hPCSK9^{TG(Alb-Cre)} mice injected with miR-NC, LDL cholesterol levels were higher than those in Alb-Cre mice, and no changes were observed in very low-density lipoprotein (VLDL) or high-density lipoprotein (HDL) levels (Figure 5C). Whole-body overexpression of human PCSK9 in mice can reduce hepatic Ldlr in mice by approximately 90%. ^{25,26} However, in liver-specific human PCSK9 overexpressing mice, hepatic Ldlr was reduced by approximately 50%, and hsa-miR-1912-3p injection enhanced Ldlr expression (Figures 5B and 5C). In addition, the increased levels of LDL cholesterol in hPCSK9^{TG(Alb-Cre)} mice were reduced to the levels observed in Alb-Cre mice upon tail vein injection of hsa-miR-1912-3p, with no significant differences in the levels of VLDL and HDL cholesterol (Figure 5C). These results suggest that hsa-miR-1912-3p effectively controls dyslipidaemia by regulating the expression of PCSK9.

DISCUSSION

The purpose of this study was to identify miRNAs that regulate PCSK9 expression and investigate whether these miRNAs affect cellular cholesterol homeostasis. This study demonstrated that among several miRNAs targeting *PCSK9*, hsa-miR-1912-3p most effectively reduced PCSK9 expression and altered blood cholesterol levels in animal models. *In vitro*, the 3' UTR luciferase assay verified that hsa-miR-1912-3p specifically acts on the *PCSK9-3*'-UTR. Furthermore, animal experiments using human *PCSK9-3*'-UTR TG mice confirmed that exogenously administered hsa-miR-1912-3p inhibited the expression of PCSK9.

The miRbase database provides all miRNA sequences and information about novel miRNAs using small RNA deep sequencing datasets.²⁷ In addition, multiple bioinformatics algorithms are available on the internet for the identification of miRNAs that target specific genes.^{28,29} These are the most useful tools for predicting miRNA targets. However, each algorithm often yields different prediction results for miRNA candidates of a single gene. Therefore, each algorithm may predict distinct miRNA-binding sites and analyze the probability of miRNA-mRNA interactions differently. Therefore, it is recommended that at least two algorithms have higher predictive accuracy.³⁰

In this study, two algorithms, TargetScan and miRanda, were used to predict the miRNAs targeting *PCSK9*. As expected, both algorithms identified hundreds of miRNAs, and their lists differed to a certain degree. Based on the probability score of functional miRNA-mRNA interactions, the top 10 ranked miRNAs of both algorithms were compared, and overlapping miRNAs were selected as potential regulators of PCSK9 for additional validation experiments.

The specificity of miRNA target selection is affected by various unknown factors besides seed pairing.³¹ Therefore, experimental validation is needed to confirm whether the predicted miRNAs are functional in certain biological processes. For example, hsa-miR-99b, the top-ranked miRNA targeting *PCSK9* in TargetScan, did not alter the expression of PCSK9 (Figure 1C). Hence, among the selected miR-NAs, hsa-miR-224-5p and hsa-miR-1912-3p were selected based on immunoblot results.

Alessandro et al. showed that PCSK9 and IDOL, proteins that regulate the expression of LDLR, are regulated by miR-224, and overexpression of hsa-miR-224-5p in LDLR^{+/-} mice reduced blood cholesterol by 15%.²³ Our results showed that treatment with hsamiR-224-5p and hsa-miR-1912-3p in HepG2 cells significantly altered the expression of genes involved in lipid metabolism compared to the control (see Figure S3). has-miR-1912-3p increased the expression of LDLR and decreased the expression of PCSK9 more strongly than hsa-miR-224-5p did (Figures 3A and 3B). Furthermore, for a combination of hsa-miR-224-5p and hsa-miR-1912-3p, the reduction in PCSK9 was less than with hsa-miR-1912-3p alone, and LDLR expression only increased in the presence of hsa-miR-1912-3p (Figure S6). In in vitro experiments, hsa-miR-1912-3p increased LDLR mRNA, but it is difficult to explain this change by the mechanism that hsa-miR-1912-3p suppresses the expression of PCSK9. PCSK9 is known to be involved in the post-translational regulation of LDLR, and its regulatory mechanism at the transcription level has not yet been elucidated. Alternatively, it is possible that hsamiR-1912-3p increases LDLR mRNA by a mechanism that does not involve PCSK9, independent of reducing PCSK9. Intracellular cholesterol metabolism is regulated by the amount of intracellular cholesterol and the expression and feedback mechanisms of several proteins, including the transcription factor SREBP-2 and its downstream proteins PCSK9 and LDLR. The increase in LDLR mRNA by hsa-miR-1912-3p may be influenced by the complex and fine regulation of intracellular cholesterol homeostasis. Nevertheless, it seems clear that hsa-miR-1912-3p goes beyond this complex metabolic process to increase LDL-cholesterol in cells via LDLR. In addition, in human PCSK9-3'-UTR gene TG mice, exogenously administered hsa-miR-1912-3p effectively reduced the protein level of

A supplemented with $2 \mu g/mL$ Dil-LDL. After 3 h of incubation, the cells were washed twice with PBS, and fluorescence microscopic images were taken. Scale bars, $20 \mu m$. (G and H) After microscopic image acquisition, the cells were trypsinized, suspended in PBS, and analyzed using a flow cytometer. The mean fluorescence intensity (MFI) of 10^4 cells was analyzed using a histogram and quantified. Histograms represent the distribution of the fluorescence intensities of Dil-LDL in cells transfected with miRNA mimics (red line). Diagrams show the MFI of Dil-LDL in cells transfected with miRNA mimics relative to that in cells transfected with miR-NC (n = 3/group). Statistics were performed using one-way ANOVA with Tukey's *post hoc* test or using ordinary two-way ANOVA with Dunnett's multiple comparison test. Each value represents the mean \pm SD (*p < 0.05, **p < 0.01, ***p < 0.001, and ****p < 0.001; n.s, not significant).

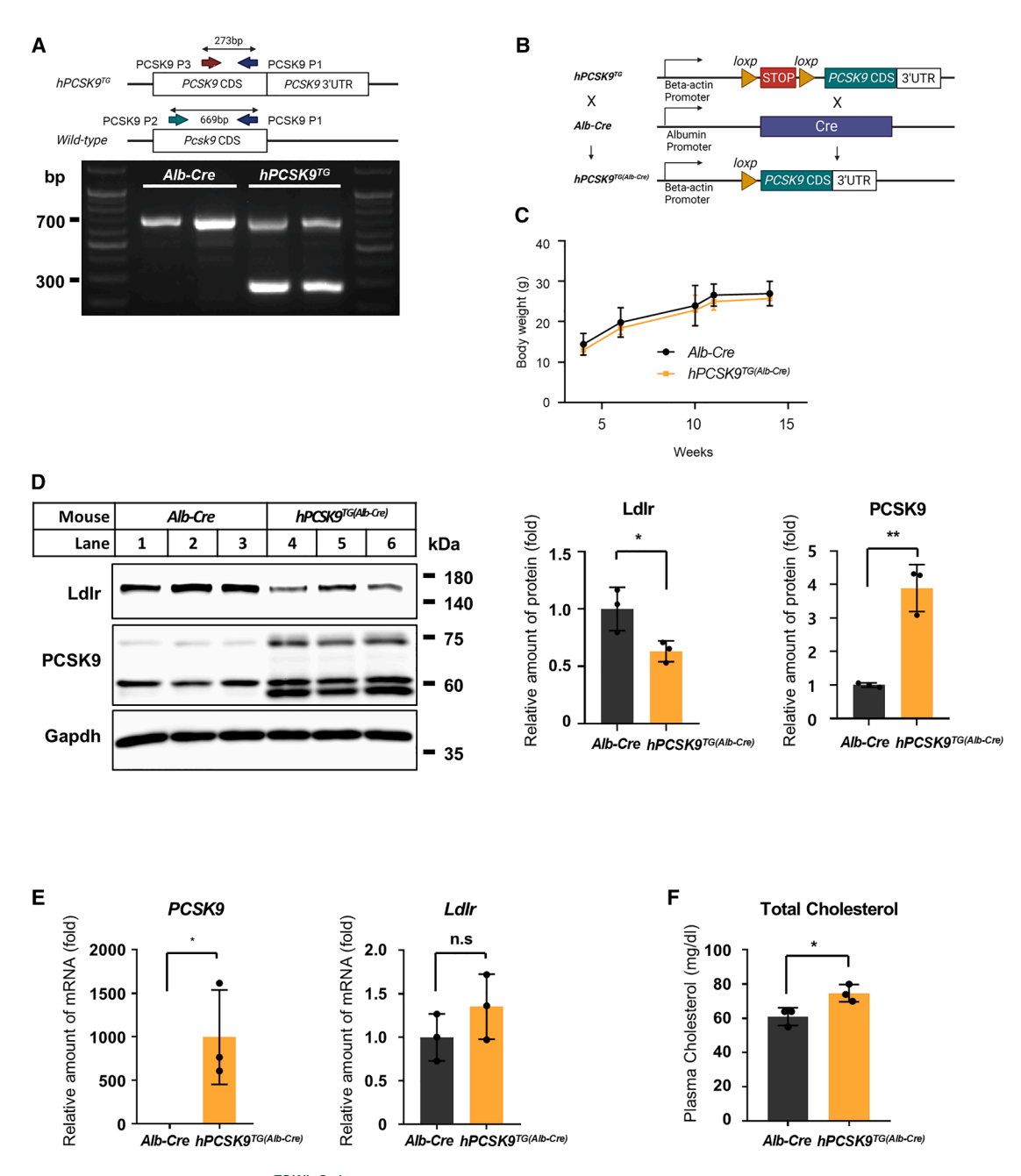


Figure 4. Baseline characteristics of $hPCSK9^{TG(Alb-Cre)}$ mice

(A) Schematic illustration of genotyping of $hPCSK9^{TG}$ mice. Genomic DNA isolated from $hPCSK9^{TG}$ and Alb-Cre mice was analyzed by PCR. (B) Schematic representation of the generation of liver-specific $hPCSK9^{TG}$ ($hPCSK9^{TG}$ ($hPCSK9^{TG}$ ($hPCSK9^{TG}$ ($hPCSK9^{TG}$ ($hPCSK9^{TG}$). (C) The body weights of wild-type male mice and 8 $hPCSK9^{TG}$ male mice are shown. (n = 3/group) (D) Proteins were isolated from the livers of wild-type and $hPCSK9^{TG}$ mice, and immunoblot analysis was performed using polyclonal antibodies against PCSK9 and LDLR. GAPDH was used as a loading control. (E) Total RNAs from the livers of wild-type and $hPCSK9^{TG}$ mice were prepared and subjected to reverse transcription and RT-qPCR. Primers used for RT-qPCR are listed in Table S2. A two-tailed unpaired Student's t test was performed for two-group comparison. Each value represents the mean \pm SD (*p < 0.05). (F) Plasma was collected from the blood of five wild-type and five $hPCSK9^{TG/Alb-Cre)}$ male mice, and the amount of total cholesterol was measured using a colorimetric method. Statistics were performed using a two-tailed unpaired Student's t test with a Shapiro-Wilk test. Each value represents the mean \pm SEM (*p < 0.05) and **p < 0.01; n.s, not significant).

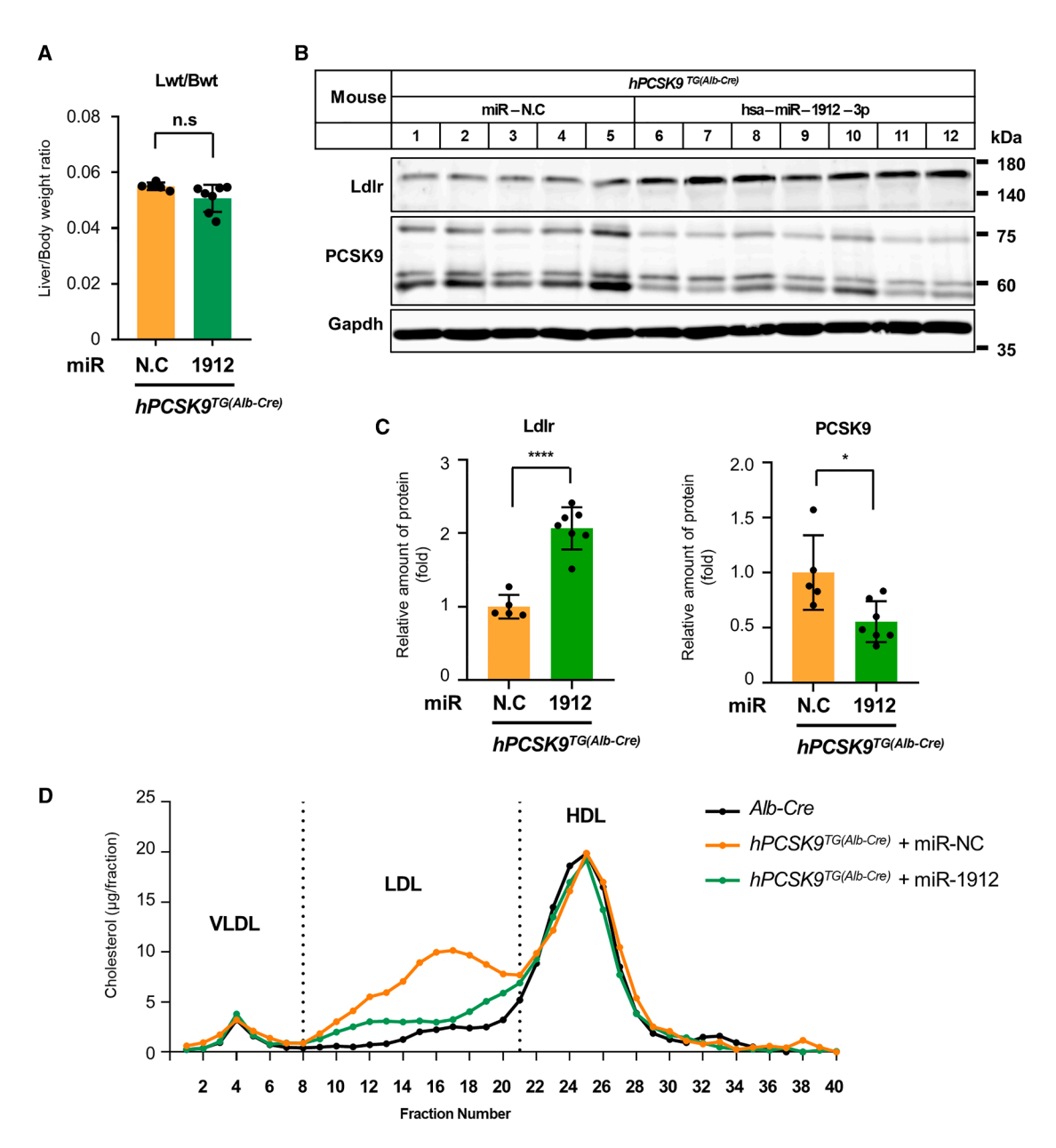


Figure 5. miR-1912 reduces the expression of hPCSK9 in vivo

(A) The ratio of liver weight to body weight of $hPCSK9^{TG(Alb-Cre)}$ mice administered with miR-NC (4 mg/kg) or miR-1912 (4 mg/kg) for 24 h. Values are expressed as the mean \pm SD of five mice per group. Statistical analyses were performed using one-way analysis of variance (n=5 for miR-NC/n=7 for miR-1912). A two-tailed unpaired Student's t test was performed for two-group comparison. Each value represents the mean \pm SD (*p < 0.05). (B) Protein was isolated from the livers of $hPCSK9^{TG(Alb-Cre)}$ mice injected with miR-NC or miR-1912, and immunoblot analysis was performed. (C) Quantitative graph of densitometry analysis for LdIr and PCSK9 images in Figure 5B. Data were normalized to GAPDH and quantified relative to the miR-NC treatment group. (D) Plasma from wild-type (black dot) and $hPCSK9^{TG(Alb-Cre)}$ male mice injected with miR-NC (orange dot) or miR-1912 (green dot) was pooled and subjected to ultracentrifugation. The lipoprotein fractions were separated by FPLC gel filtration, and the cholesterol content of each fraction was measured using an enzymatic assay. VLDL (fractions 1–8), LDL (fractions 8–21), and HDL (fractions 21–40). Statistics were performed using a two-tailed unpaired Student's t test with a Shapiro-Wilk test. Each value represents the mean \pm SEM (*p < 0.05 and *****p < 0.0001; n.s., not significant).

PCSK9 and reduced blood cholesterol, which experimentally demonstrated the mechanism of PCSK9 regulation and blood cholesterol control by hsa-miR-1912-3p *in vivo* more clearly than the previous hsa-miR-224-5p experiment.

A recent study reported that miR-483 reduces hypercholesterolemia by inhibiting PCSK9 production.³² Dong et al. reported that pre-miR-1912 failed to reduce luciferase activity with the human *PCSK9*-3'-UTR; however, in our experiments, hsa-miR-1912-3p not only

reduced luciferase activity but also reduced the *PCSK9* transcript and decreased the protein expression of PCSK9. Although it was not compared to miR-483, hsa-miR-1912-3p increased LDLR expression and LDL uptake in HepG2 cells. The reason for the discrepancy between our results and those of the previous study is unclear, but one possible explanation is that the previous study used pre-miRs, whereas we used mature miRs. Jianjie et al. comprehensively demonstrated the mechanism of action of miR-483 *in vivo* by introducing the mouse *PCSK9* gene and miR-483 into mice using adeno-associated viruses. In contrast, the strength of our study is that we created a humanized mouse model in which the human *PCSK9* gene, including the 3' UTR, was inserted into the mice's genome and confirmed that miR-1912 effectively reduced the expression of human *PCSK9* without hepatoxicity, suggesting that hsa-miR-1912-3p can be used to inhibit PCSK9 and reduce blood cholesterol levels in the human body.

has-miR-1912-3p is located in intron 2 of *HTR2C* and expresses exclusively in neuronal cells.³³ It is quite an impressive result that hsamiR-1912-3p had a great effect on cholesterol metabolism, significantly decreasing PCSK9 and increasing LDLR. However, the effect of endogenous hsa-miR-1912-3p on cholesterol metabolism was not examined in this study because hsa-miR-1912-3p was not expressed in HepG2 cells. To date, the expression of hsa-miR-1912-3p has been confirmed in the brain cortex and primary lymphocytes.³⁴ At first, PCSK9 was identified as a molecule involved in neuronal differentiation.³⁵ Therefore, it is conceivable that hsa-miR-1912-3p is related to tissue-specific or species-specific regulation of cholesterol metabolism. For example, hsa-miR-1912-3p may play a role in nervous system differentiation by regulating the expression of PCSK9 and controlling cellular cholesterol levels.

Both miRNAs and siRNAs silence target genes, but they differ in their mechanism of action, with miRNAs originating from an organism's genome and siRNAs being produced exogenously by chemical synthesis.³⁶ The PCSK9 siRNA, inclisiran, has been shown to safely and effectively reduce blood cholesterol levels in a large human clinical trial, and compared to placebo, inclisiran reduced major adverse cardiovascular events by 26%.³⁷ Despite the successful development of siRNA agents, the development of therapeutic agents using miR-NAs has been very rare due to concerns about off-target effects, as miRNAs have relatively more flexible complementary binding to target mRNAs than siRNAs.³⁸ In the microarray results of hsa-miRNA-1912-3p-transfected HepG2 cells, the modulation of various genes suggests that hsa-miR-1912-3p may influence LDLR expression not only through the regulation of PCSK9 mRNA but also by affecting other genes involved in lipid metabolism. One limitation of this study is the lack of investigation into the mechanism of action of hsamiR-1912-3p in normal human cells, such as human primary hepatocytes. And, due to the sequence mismatch between human and mouse miR-1912, we did not conduct in vivo transcriptomic analysis in mice. Therefore, we cannot rule out the possibility that hsa-miR-1912-3p may have additional biological effects beyond PCSK9 suppression in humans. Further studies are needed to explore these mechanisms in greater detail and on the long-term physiological effects of the hsa-miR-1912-3p. In our study, the lack of difference in weight and survival after hsa-miRNA-1912-3p treatment compared to the control suggests that hsa-miR-1912-3p safely reduces human PCSK9 expression; however, its role and safety under physiological conditions remain to be elucidated.

Conclusions

Our study screened miRNAs that can regulate PCSK9 using bioinformatics and showed that hsa-miR-1912-3p was the most potent inhibitor of PCSK9 expression, leading to an increase in cellular LDLR and a corresponding increase in cellular LDL cholesterol uptake. Furthermore, administration of hsa-miR-1912-3p reduced the expression of PCSK9 in the liver of mice and reduced blood LDL-cholesterol. This suggests that *in vivo* miRNA-mediated regulation of cholesterol may be a novel therapeutic option for hypercholesterolemia.

MATERIALS AND METHODS

Materials

Delipidated serum (DLPS) was prepared from fetal bovine serum (FBS) as described by Hannah et al.³⁹ Protein concentrations were determined using a bicinchoninic acid kit (Pierce, Rockford, IL, USA). Cell culture medium and reagents were obtained from Invitrogen (Carlsbad, CA, USA). N-Acetyl-leucine-leucine-norleucinal was obtained from Merck Biosciences (Calbiochem, San Diego, CA, USA). Rosuvastatin was provided by AstraZeneca (Mölndal, Sweden). Sodium mevalonate was prepared using mevalonic acid lactone (Sigma-Aldrich Co., St. Louis, MO, USA) as previously described. 40 mirVana negative control (miR-NC, cat no. 4464059), mirVana miRNA mimics, and mirVana miRNA inhibitors were purchased from Ambion Inc. (Bedford, MA, USA) and their information was displayed in Table S1. Dil-LDL was purchased from Biomedical Technologies, Inc. (Stoughton, MA, USA). All other unspecified reagents were purchased from Sigma-Aldrich. The anti-GAPDH antibody was purchased from Cell Signaling Technology, Inc. (Beverly, MA, USA). Horseradish peroxidase-conjugated secondary antibodies were purchased from Pierce. Polyclonal antibodies against PCSK9 were prepared as previously described by Jeong et al.⁹ The polyclonal antibodies against human LDLR were raised in rabbits using C-bLDLR conjugated with keyhole limpet hemocyanine synthetic peptides spanning amino acids 832-841 of bovine LDLR according to the standard technique.41

Generation of liver-specific human PCSK9-3'-UTR transgenic mice

To generate conditional human *PCSK9-3'*-UTR transgenic (*hPCSK9^{TG}*) mice, full-length cDNA of human *PCSK9-3'*-UTR was subjected to polymerase chain reaction (PCR) amplification from the HepG2 cDNA library and cloned into the pCB vector (see Figure S3A). The cloned plasmid was linearized using restriction enzymes and microinjected into C57BL/6 mouse embryos. Microinjections were performed as previously described. The *hPCSK9^{TG}* mice were generated by GEMCRO Inc. (Seoul, Korea). The *hPCSK9^{TG}* mice were crossbred with *Alb-Cre* mice to generate *Alb-Cre/hPCSK9-3'*-UTR TG (*hPCSK9^{TG(Alb-Cre)}*) mice. *Alb-Cre* mice were

kindly provided by Professor Han Woong Lee (Yonsei University, Seoul, Republic of Korea). The protein expressions of LDLR and PCSK9 in WT, PCSK9 knockout, Alb-Cre, and PCSK9 TG mice are shown in Figure S3B. All mice were maintained on a 12-h light/dark cycle with ad libitum access to food and water. All animal experiments were approved by the Institutional Animal Care and Use Committee (IACUC) of Yonsei University Health System (protocol nos: 2017-0177 and 2019-0193). This study adhered to the guidelines outlined in the Guide for the Care and Use of Laboratory Animals (8th Edition, 2011) by the National Research Council of the National Academies, and it complied with the standards set by the Association for Assessment and Accreditation of Laboratory Animal Care International.

Injection of miRNA in human $hPCSK9^{TG(A/b-Cre)}$ mice and organ harvest

Eight-week-old male PCSK9^{TG(Alb-Cre)} mice were injected with 4 mg/kg of miR-NC or miR-1912 complexed with in vivo jetPEI (Polyplus Transfection, Strasbourg, France), following the manufacturer's instructions by tail vein. Mice were starved at 16 h after injection and anesthetized 24 h after the injection. Pre-euthanasia sedation for liver and blood harvest was performed with Zoletil and Rompun. Briefly, the mice were anesthetized with Zoletil (tiletamine/zolazepam; 30 mg/kg) and Rompun (xylazine; 15 mg/kg) by intraperitoneal injection. Blood samples were collected in the presence of 2 mM EDTA and aprotinin from the inferior vena cava for plasma preparation, and the livers were frozen in liquid nitrogen for immunoblot and RT-qPCR analysis. To verify miRNA delivery to the liver, miRNA was purified using the miRNeasy Micro Kit (-QIAGEN, Hilden, Germany), according to the manufacturer's instructions and quantified by TaqMan assay (Figure S7A). After organ harvest, cervical dislocation was performed for euthanasia.

Cell culture and transfection

HepG2 cells (American Type Culture Collection, HB-8065) were maintained in medium A (DMEM containing 100 U/mL penicillin and 100 µg/mL streptomycin sulfate) supplemented with 10% (v/v) FBS. Transfection of miRNA mimics or miRNA inhibitors into HepG2 cells in suspension was carried out using Lipofectamine 2000 (Invitrogen) according to the method described by Notarangelo et al. with minor modifications. 43 Briefly, miRNA mimics or miRNA inhibitors were complexed in Opti-MEM (Invitrogen) using Lipofectamine 2000 according to the manufacturer's instructions. When the miRNA mimic or inhibitor-lipofectamine complex was prepared, HepG2 cells were trypsinized and suspended in medium A supplemented with 10% FBS. The complex was mixed with 2×10^5 cells per well/12-well plate in 0.8 mL of medium A supplemented with 10% FBS and rocked gently for 20 min at 37°C. Aliquots of the mixtures were plated in 12-well plates and cultured overnight at 37°C under a humidified atmosphere of 5% CO₂. On day 1, the cells were washed twice with PBS and changed to medium A supplemented with 10% DLPS, 0.1 µM rosuvastatin, and 50 µM sodium mevalonate in the absence or presence of 1 μg/mL 25-hydroxycholesterol plus 10 μg/mL cholesterol added to a final concentration of 0.2% (v/v) ethanol. On day 2, cells were washed twice with PBS and harvested for

further analysis. To verify miRNA delivery to cell, miRNA was isolated using the miRNeasy Micro Kit (QIAGEN), following to the manufacturer's instructions and quantified by TaqMan assay (Figure S7B). Transfection of plasmids into HEK293 cells was performed using Lipofectamine 2000 (Invitrogen) according to the manufacturer's instructions.

RNA isolation and qRT-PCR

Total RNA, including the miRNA fraction, was isolated using the miR-Neasy Micro Kit (QIAGEN), according to the manufacturer's instructions. DNA was removed from the RNA using RNase-free DNase (QIAGEN). For mRNA quantification, cDNA was synthesized from 2 μg of DNase-treated RNA using a High Capacity cDNA Synthesis Kit (Applied Biosystems, Foster City, CA, USA). qRT-PCR was performed using PowerSYBR Green PCR Master Mix (Applied Biosystems). All reactions were analyzed using the StepOne Real-Time PCR system (Applied Biosystems). GAPDH was used as a reference for the mRNA expression analysis. Each sample was analyzed in triplicate, and the relative amounts were quantified using the comparative cycle-time method. The primers used for qRT-PCR are listed in Table S2. For miRNA qRT-PCR, RNA purified from either mouse liver or HepG2 cells was reverse transcribed to cDNA using the TaqMan MicroRNA Reverse Transcription Kit (Invitrogen) according to the manufacturer's instructions, with snoRNA (assay ID: 001232) and U6 snRNA (assay ID: 001973) used for normalization in the respective samples. cDNA for hsa-miR-1912-3p (assay ID: 478737_mir) was synthesized using the TaqMan Advanced miRNA cDNA Synthesis Kit (Invitrogen) according to the manufacturer's instructions, and the assay was performed. qRT-PCR of the synthesized cDNAs was carried out using the TaqMan Fast Advanced Master Mix for qPCR (Applied Biosystems) following the manufacturer's instructions and quantified using $\Delta\Delta$ Ct method.

Immunoblot analysis

After treatment of cells as described in each figure legend, cells were washed twice with PBS and lysed with 200 µL of lysis buffer containing 0.33 M NaCl, 1.1 M urea, 1% Nonidet P-40, 25 mM HEPES, pH 7.6 (NUN buffer), and protein inhibitors (1 mM DTT, 10 µg/mL leupeptin, 1 mM phenylmethanesulfonyl trifluoride (PMST), 2 μg/mL aprotinin, and 50 µg/mL N-acetyl-leucine-leucine-norleucinal) by adding directly onto the plate. 44 Cell lysates were harvested and further vortexed at room temperature for 10 min for the complete liberation of proteins. The lysates were cleared by centrifugation at $20,000 \times g$ for 15 min at 4°C, and the supernatants were collected as whole-cell lysates. After protein quantification, aliquots of the proteins were subjected to 8% SDS-PAGE, transferred onto nitrocellulose-enhanced chemiluminescence membranes (GE Healthcare, Piscataway, NJ, USA), and immunoblot analyses were performed using the SuperSignal West Pico Chemiluminescent Substrate System (Pierce).

Screening of miRNAs targeting PCSK9

The 3' UTR sequence of human *PCSK9* mRNA was retrieved using Entrez (http://www.ncbi.nlm.nih.gov/entrez/). The sequence was

then analyzed to identify the binding sites for potential miRNAs targeting human *PCSK9* using the online computational algorithms TargetScan Release 6.0 (https://www.targetscan.org/vert_60/) and miRanda (http://www.microrna.org).

Luciferase reporter assay

The PCSK9-3'-UTR luciferase reporter (pLightSwitch_PC-SK9_3UTR) construct harboring the complete 3' UTR of the human PCSK9 mRNA downstream of the Renilla luciferase gene was purchased from Switchgear Genomics (Menlo Park, CA, USA). Site-directed mutagenesis of the putative seed regions in the 3' UTR of miRNAs was performed using pfu DNA polymerase (Agilent Technologies, Palo Alto, CA, USA) to create mutant variants of the PCSK9-3'-UTR luciferase reporter construct. Primer sequences and genomic locations used for mutagenesis are listed in Table S4. For luciferase reporter assays, HEK293 cells were plated in a 24-well plate and then co-transfected with 80 ng of firefly luciferase control vector (pGL3-control, Promega, Madison, WI, USA), 200 ng of the 3' UTR luciferase reporter construct, and 40 nM (final concentration) of miRNA mimic using Lipofectamine 2000 (Invitrogen) according to the manufacturer's instructions. Cells were lysed 48 h after transfection, and luciferase activity was measured using the Dual-Luciferase Reporter Assay System (Promega). pGL3-control was co-transfected with the construct as an internal control to standardize the transfection efficiency. Renilla luciferase activity representing the activity of the 3' UTR of PCSK9 mRNA was normalized to the firefly luciferase activity driven by the pGL3-control vector and the amount of protein in the lysate. Transfections were performed in duplicate and repeated at least thrice in independent experiments.

AGO2 pull-down assay

To induce mRNA of *PCSK9* and *LDLR*, HepG2 cells were prepared using a modified version of the transfection method described previously. Briefly, on day 0, HepG2 cells were treated for 24 h with DMEM supplemented with 10% DLPS and 1% P/S media. On day 1, the cells were treated for 16 h with DMEM supplemented with 10% DLPS and 1% P/S containing 0.05 mM sodium mevalonate and 0.1 μ M rosuvastatin. Subsequently, 5 \times 10 6 HepG2 cells were transfected with 0, 10, 20, and 40 nM of hsa-miR-1912-3p for 24 h using Lipofectamine 2000 according to the manufacturer's instructions. Then, the AGO2 pull-down assay was performed following a previously published protocol. 45 The AGO2 antibody used for the pull-down was the AGO2 monoclonal antibody (AGO2 11A9, Invitrogen), and the primers used for RT-qPCR are listed in the Table S2.

Fluorescence microscopy and the LDL uptake assay

After 24 h of transfection of HepG2 cells with miR-NC, miR-224, or miR-1912, cells were incubated with 10% DLPS culture medium for 24 h, followed by treatment for 3 h with 2 μ g/mL of fluorescence-labeled Dil-LDL. After washing the cells with PBS, fluorescence images were obtained using a fluorescence microscope (Olympus, Tokyo, Japan) with a rhodamine filter. To quantify LDL uptake, the cells were trypsinized to obtain a single-cell suspension. The mean fluo-

rescence intensity of 10,000 cells was analyzed by FACS using a FACScan (BD Biosciences, San Jose, CA, USA).

FPLC analysis

Pooled plasma (300 $\mu L)$ from three male mice of each genotype was subjected to gel filtration with FPLC as previously described. 46 Fractions (1 mL) were collected, and 0.2 mL from each fraction was used to determine the content of total cholesterol and triglycerides.

Statistical analysis

Three experiments were performed in all the *in vitro* studies. The results are presented as the mean ± standard deviation (SD). The data were analyzed using a two-tailed Student's t test, and sample normality was confirmed by the Shapiro-Wilk test. For multiple-group analysis, a one-way ANOVA was used to determine significant differences, followed by Tukey's *post hoc* test. Mouse experiment results are expressed as the mean ± SEM and are analyzed by a two-tailed Student's t test. Statistical analysis of survival curves was performed with a log rank test. Statistical analyses were performed using SPSS version 18.0 for Windows (Statistical Package for the Social Sciences, SPSS, Inc., Chicago, IL, USA) and GraphPad Prism version 8.0.1.

DATA AVAILABILITY

All raw data supporting the findings from this study are available from the corresponding authors upon request. All microarray datasets analyzed in this study are available from Gene Expression Omnibus (GEO) accession: GSE262184.

ACKNOWLEDGMENTS

We thank Jaehoon Lee and Han-Woong Lee (Department of Biochemistry, College of Life Science and Biotechnology, Yonsei University, and GEMCRO Inc.) for generating transgenic mice. The graphical abstract was generated with BioRender. This study was supported partly by the Virtual Research Institute Project, 2012, hosted by AstraZeneca (United Kingdom) and the Korea Health Industry Development Institute (KHIDI), the Korean government Ministry of Science and ICT (grant no. 2020R1C1C1013627), and the Korea Health Technology R&D Project through the KHIDI, funded by the Ministry of Health & Welfare, the Republic of Korea (RS-2023-00305184).

AUTHOR CONTRIBUTIONS

C.J.L. and S.W.P. designed the study. S.W.P. and S.L. supervised the study. C.J.L. and M. G. wrote the manuscript and performed the experiments. S.W.P., S.L., and C.J.L. interpreted the data. M.G and S.-B.J. performed animal experiments. S.-H.L. performed FPLC and interpreted the data. D.M. attributed to generate Tg mouse. S.H.P. attributed to reviewing and editing manuscript and figures.

DECLARATION OF INTERESTS

The authors declare no competing interests.

SUPPLEMENTAL INFORMATION

Supplemental information can be found online at https://doi.org/10.1016/j.omtn.2025. 102589.

REFERENCES

- Goldstein, J.L., Brown, M.S., Anderson, R.G., Russell, D.W., and Schneider, W.J. (1985). Receptor-mediated endocytosis: concepts emerging from the LDL receptor system. Annu. Rev. Cell Biol. 1, 1–39. https://doi.org/10.1146/annurev.cb.01. 110185.000245.
- Gent, J., and Braakman, I. (2004). Low-density lipoprotein receptor structure and folding. Cell. Mol. Life Sci. 61, 2461–2470. https://doi.org/10.1007/s00018-004-4090-3.

- Zhang, D.W., Lagace, T.A., Garuti, R., Zhao, Z., McDonald, M., Horton, J.D., Cohen, J.C., and Hobbs, H.H. (2007). Binding of proprotein convertase subtilisin/kexin type 9 to epidermal growth factor-like repeat A of low density lipoprotein receptor decreases receptor recycling and increases degradation. J. Biol. Chem. 282, 18602– 18612. https://doi.org/10.1074/jbc.M702027200.
- Abifadel, M., Varret, M., Rabès, J.P., Allard, D., Ouguerram, K., Devillers, M., Cruaud, C., Benjannet, S., Wickham, L., Erlich, D., et al. (2003). Mutations in PCSK9 cause autosomal dominant hypercholesterolemia. Nat. Genet. 34, 154–156. https://doi.org/10.1038/ng1161.
- Cohen, J.C., Boerwinkle, E., Mosley, T.H., Jr., and Hobbs, H.H. (2006). Sequence variations in PCSK9, low LDL, and protection against coronary heart disease. N. Engl. J. Med. 354, 1264–1272. https://doi.org/10.1056/NEJMoa054013.
- Goldstein, J.L., and Brown, M.S. (2009). The LDL receptor. Arterioscler. Thromb. Vasc. Biol. 29, 431–438. https://doi.org/10.1161/ATVBAHA.108.179564.
- Dubuc, G., Chamberland, A., Wassef, H., Davignon, J., Seidah, N.G., Bernier, L., and Prat, A. (2004). Statins upregulate PCSK9, the gene encoding the proprotein convertase neural apoptosis-regulated convertase-1 implicated in familial hypercholester-olemia. Arterioscler. Thromb. Vasc. Biol. 24, 1454–1459. https://doi.org/10.1161/01.ATV.0000134621.14315.43.
- Mabuchi, H., and Nohara, A. (2015). Therapy: PCSK9 inhibitors for treating familial hypercholesterolaemia. Nat. Rev. Endocrinol. 11, 8–9. https://doi.org/10.1038/ nrendo.2014.205.
- Jeong, H.J., Lee, H.S., Kim, K.S., Kim, Y.K., Yoon, D., and Park, S.W. (2008). Sterol-dependent regulation of proprotein convertase subtilisin/kexin type 9 expression by sterol-regulatory element binding protein-2. J. Lipid Res. 49, 399–409. https://doi.org/10.1194/jlr.M700443-JLR200.
- Rashid, S., Curtis, D.E., Garuti, R., Anderson, N.N., Bashmakov, Y., Ho, Y.K., Hammer, R.E., Moon, Y.A., and Horton, J.D. (2005). Decreased plasma cholesterol and hypersensitivity to statins in mice lacking Pcsk9. Proc. Natl. Acad. Sci. USA 102, 5374–5379. https://doi.org/10.1073/pnas.0501652102.
- Sabatine, M.S., Giugliano, R.P., Keech, A.C., Honarpour, N., Wiviott, S.D., Murphy, S.A., Kuder, J.F., Wang, H., Liu, T., Wasserman, S.M., et al. (2017). Evolocumab and Clinical Outcomes in Patients with Cardiovascular Disease. N. Engl. J. Med. 376, 1713–1722. https://doi.org/10.1056/NEJMoa1615664.
- Schwartz, G.G., Steg, P.G., Szarek, M., Bhatt, D.L., Bittner, V.A., Diaz, R., Edelberg, J. M., Goodman, S.G., Hanotin, C., Harrington, R.A., et al. (2018). Alirocumab and Cardiovascular Outcomes after Acute Coronary Syndrome. N. Engl. J. Med. 379, 2097–2107. https://doi.org/10.1056/NEJMoa1801174.
- Alonso, R., Muñiz-Grijalvo, O., Díaz-Díaz, J.L., Zambón, D., de Andrés, R., Arroyo-Olivares, R., Fuentes-Jimenez, F., Muñoz-Torrero, J.S., Cepeda, J., Aguado, R., et al. (2021). Efficacy of PCSK9 inhibitors in the treatment of heterozygous familial hyper-cholesterolemia: A clinical practice experience. J. Clin. Lipidol. 15, 584–592. https://doi.org/10.1016/j.jacl.2021.04.011.
- Ray, K.K., Landmesser, U., Leiter, L.A., Kallend, D., Dufour, R., Karakas, M., Hall, T., Troquay, R.P.T., Turner, T., Visseren, F.L.J., et al. (2017). Inclisiran in Patients at High Cardiovascular Risk with Elevated LDL Cholesterol. N. Engl. J. Med. 376, 1430–1440. https://doi.org/10.1056/NEJMoa1615758.
- Bartel, D.P. (2004). MicroRNAs: genomics, biogenesis, mechanism, and function. Cell 116, 281–297. https://doi.org/10.1016/s0092-8674(04)00045-5.
- Finotti, A., Fabbri, E., Lampronti, I., Gasparello, J., Borgatti, M., and Gambari, R. (2019). MicroRNAs and Long Non-coding RNAs in Genetic Diseases. Mol. Diagn. Ther. 23, 155–171. https://doi.org/10.1007/s40291-018-0380-6.
- Miao, C., Chang, J., Zhang, G., and Fang, Y. (2018). MicroRNAs in type 1 diabetes: new research progress and potential directions. Biochem. Cell. Biol. 96, 498–506. https://doi.org/10.1139/bcb-2018-0027.
- McCoy, C.E. (2017). miR-155 Dysregulation and Therapeutic Intervention in Multiple Sclerosis. Adv. Exp. Med. Biol. 1024, 111–131. https://doi.org/10.1007/ 978-981-10-5987-2_5.
- Lee, S.W.L., Paoletti, C., Campisi, M., Osaki, T., Adriani, G., Kamm, R.D., Mattu, C., and Chiono, V. (2019). MicroRNA delivery through nanoparticles. J. Control. Release 313, 80–95. https://doi.org/10.1016/j.jconrel.2019.10.007.
- Yang, N. (2015). An overview of viral and nonviral delivery systems for microRNA. Int. J. Pharm. Investig. 5, 179–181. https://doi.org/10.4103/2230-973X.167646.

- Rayner, K.J., Suárez, Y., Dávalos, A., Parathath, S., Fitzgerald, M.L., Tamehiro, N., Fisher, E.A., Moore, K.J., and Fernández-Hernando, C. (2010). MiR-33 contributes to the regulation of cholesterol homeostasis. Science 328, 1570–1573. https://doi.org/ 10.1126/science.1189862.
- Iliopoulos, D., Drosatos, K., Hiyama, Y., Goldberg, I.J., and Zannis, V.I. (2010).
 MicroRNA-370 controls the expression of microRNA-122 and Cpt1alpha and affects lipid metabolism. J. Lipid Res. 51, 1513–1523. https://doi.org/10.1194/jlr. M004812.
- Salerno, A.G., van Solingen, C., Scotti, E., Wanschel, A.C.B.A., Afonso, M.S., Oldebeken, S.R., Spiro, W., Tontonoz, P., Rayner, K.J., and Moore, K.J. (2020). LDL Receptor Pathway Regulation by miR-224 and miR-520d. Front. Cardiovasc. Med. 7, 81. https://doi.org/10.3389/fcvm.2020.00081.
- Naeli, P., Mirzadeh Azad, F., Malakootian, M., Seidah, N.G., and Mowla, S.J. (2017).
 Post-transcriptional Regulation of PCSK9 by miR-191, miR-222, and miR-224.
 Front. Genet. 8, 189. https://doi.org/10.3389/fgene.2017.00189.
- Lagace, T.A., Curtis, D.E., Garuti, R., McNutt, M.C., Park, S.W., Prather, H.B., Anderson, N.N., Ho, Y.K., Hammer, R.E., and Horton, J.D. (2006). Secreted PCSK9 decreases the number of LDL receptors in hepatocytes and in livers of parabiotic mice. J. Clin. Investig. 116, 2995–3005. https://doi.org/10.1172/JCI29383.
- Grefhorst, A., McNutt, M.C., Lagace, T.A., and Horton, J.D. (2008). Plasma PCSK9
 preferentially reduces liver LDL receptors in mice. J. Lipid Res. 49, 1303–1311.
 https://doi.org/10.1194/jlr.M800027-JLR200.
- Kozomara, A., and Griffiths-Jones, S. (2014). miRBase: annotating high confidence microRNAs using deep sequencing data. Nucleic Acids Res. 42, D68–D73. https:// doi.org/10.1093/nar/gkt1181.
- Rajewsky, N. (2006). microRNA target predictions in animals. Nat. Genet. 38, S8–S13. https://doi.org/10.1038/ng1798.
- Doran, J., and Strauss, W.M. (2007). Bio-informatic trends for the determination of miRNA-target interactions in mammals. DNA Cell Biol. 26, 353–360. https://doi. org/10.1089/dna.2006.0546.
- Kuhn, D.E., Martin, M.M., Feldman, D.S., Terry, A.V., Jr., Nuovo, G.J., and Elton, T. S. (2008). Experimental validation of miRNA targets. Methods 44, 47–54. https://doi.org/10.1016/j.ymeth.2007.09.005.
- Didiano, D., and Hobert, O. (2006). Perfect seed pairing is not a generally reliable predictor for miRNA-target interactions. Nat. Struct. Mol. Biol. 13, 849–851. https://doi.org/10.1038/nsmb1138.
- 32. Dong, J., He, M., Li, J., Pessentheiner, A., Wang, C., Zhang, J., Sun, Y., Wang, W.T., Zhang, Y., Liu, J., et al. (2020). microRNA-483 ameliorates hypercholesterolemia by inhibiting PCSK9 production. JCI Insight 5, e143812. https://doi.org/10.1172/jci.insight.143812.
- Pasqualetti, M., Ori, M., Castagna, M., Marazziti, D., Cassano, G.B., and Nardi, I. (1999). Distribution and cellular localization of the serotonin type 2C receptor messenger RNA in human brain. Neuroscience 92, 601–611. https://doi.org/10.1016/s0306-4522(99)00011-1.
- 34. Zhang, Z., Falaleeva, M., Agranat-Tamir, L., Pages, A., Eyras, E., Sperling, J., Sperling, R., and Stamm, S. (2013). The 5' untranslated region of the serotonin receptor 2C pre-mRNA generates miRNAs and is expressed in non-neuronal cells. Exp. Brain Res. 230, 387–394. https://doi.org/10.1007/s00221-013-3458-8.
- Seidah, N.G., Benjannet, S., Wickham, L., Marcinkiewicz, J., Jasmin, S.B., Stifani, S., Basak, A., Prat, A., and Chretien, M. (2003). The secretory proprotein convertase neural apoptosis-regulated convertase 1 (NARC-1): liver regeneration and neuronal differentiation. Proc. Natl. Acad. Sci. USA 100, 928–933. https://doi.org/10.1073/ pnas.0335507100.
- Lam, J.K.W., Chow, M.Y.T., Zhang, Y., and Leung, S.W.S. (2015). siRNA Versus miRNA as Therapeutics for Gene Silencing. Mol. Ther. Nucleic Acids 4, e252. https://doi.org/10.1038/mtna.2015.23.
- Ray, K.K., Raal, F.J., Kallend, D.G., Jaros, M.J., Koenig, W., Leiter, L.A., Landmesser, U., Schwartz, G.G., Lawrence, D., Friedman, A., et al. (2023). Inclisiran and cardiovascular events: a patient-level analysis of phase III trials. Eur. Heart J. 44, 129–138. https://doi.org/10.1093/eurheartj/ehac594.
- Zhang, S., Cheng, Z., Wang, Y., and Han, T. (2021). The Risks of miRNA Therapeutics: In a Drug Target Perspective. Drug Des. Devel. Ther. 15, 721–733. https://doi.org/10.2147/DDDT.S288859.

- Hannah, V.C., Ou, J., Luong, A., Goldstein, J.L., and Brown, M.S. (2001).
 Unsaturated fatty acids down-regulate srebp isoforms 1a and 1c by two mechanisms in HEK-293 cells. J. Biol. Chem. 276, 4365–4372. https://doi.org/10.1074/jbc. M007273200.
- Marquart, T.J., Allen, R.M., Ory, D.S., and Baldán, A. (2010). miR-33 links SREBP-2 induction to repression of sterol transporters. Proc. Natl. Acad. Sci. USA 107, 12228– 12232. https://doi.org/10.1073/pnas.1005191107.
- Russell, D.W., Schneider, W.J., Yamamoto, T., Luskey, K.L., Brown, M.S., and Goldstein, J.L. (1984). Domain map of the LDL receptor: sequence homology with the epidermal growth factor precursor. Cell 37, 577–585. https://doi.org/10.1016/ 0092-8674(84)90388-x.
- 42. Lee, J., Kim, H.J., Moon, J.A., Sung, Y.H., Baek, I.J., Roh, J.I., Ha, N.Y., Kim, S.Y., Bahk, Y.Y., Lee, J.E., et al. (2011). Transgenic overexpression of p23 induces spontaneous hydronephrosis in mice. Int. J. Exp. Pathol. 92, 251–259. https://doi.org/10.1111/j.1365-2613.2011.00762.x.

- Notarangelo, A., Latino, R., Gasparini, P., Zelante, L., Fazio, V.M., and Rinaldi, M. (1997). Efficient transfection of adherent cells using cell suspensions. Focus 3, 58–59.
- Lavery, D.J., and Schibler, U. (1993). Circadian transcription of the cholesterol 7 alpha hydroxylase gene may involve the liver-enriched bZIP protein DBP. Genes Dev. 7, 1871–1884. https://doi.org/10.1101/gad.7.10.1871.
- Ansari, A., Yadav, P.K., Zhou, L., Prakash, B., Ijaz, L., Christiano, A., Ahmad, S., Rimbert, A., and Hussain, M.M. (2025). Casz1 and Znf101/Zfp961 differentially regulate apolipoproteins A1 and B, alter plasma lipoproteins, and reduce atherosclerosis. JCI Insight 10, e182260. https://doi.org/10.1172/jci.insight.182260.
- Min, D.K., Lee, H.S., Lee, N., Lee, C.J., Song, H.J., Yang, G.E., Yoon, D., and Park, S.
 W. (2015). In silico Screening of Chemical Libraries to Develop Inhibitors That Hamper the Interaction of PCSK9 with the LDL Receptor. Yonsei Med. J. 56, 1251–1257. https://doi.org/10.3349/ymj.2015.56.5.1251.